How Many Kilonovae Can Be Found in Past, Present, and Future Survey Data Sets?

D. Scolnic[1], R. Kessler[1], D. Brout[2], P. S. Cowperthwaite[3], M. Soares-Santos[4,5], J. Annis[4], K. Herner[4], H.-Y. Chen[1], M. Sako[2], Z. Doctor[1], R. E. Butler[4,6], A. Palmese[7], H. T. Diehl[4], J. Frieman[1,4], D. E. Holz[1,89], E. Berger[3], R. Chornock[10], V. A. Villar[3], M. Nicholl[3], R. Biswas[11,12], R. Hounsell[13,14], R. J. Foley[13], J. Metzger[1], A. Rest[15,16], J. García-Bellido[17], A. Möller[18,19], P. Nugent[20], T. M. C. Abbott[21], F. B. Abdalla[7,22], S. Allam[4], K. Bechtol[23], A. Benoit-Lévy[7,24,25], E. Bertin[24,25], D. Brooks[7], E. Buckley-Geer[4], A. Carnero Rosell[26,27], M. Carrasco Kind[28,29], J. Carretero[30], F. J. Castander[31], C. E. Cunha[32], C. B. D'Andrea[2], L. N. da Costa[26,27], C. Davis[32], P. Doel[7], A. Drlica-Wagner[4], T. F. Eifler[33,34], B. Flaugher[4], P. Fosalba[31], E. Gaztanaga[31], D. W. Gerdes[35,36], D. Gruen[32,37], R. A. Gruendl[28,29], J. Gschwend[26,27], G. Gutierrez[4], W. G. Hartley[7,38], K. Honscheid[39,40], D. J. James[41], M. W. G. Johnson[29], M. D. Johnson[29], E. Krause[32], K. Kuehn[42], S. Kuhlmann[43], O. Lahav[7], T. S. Li[4], M. Lima[26,44], M. A. G. Maia[26,27], M. March[2], J. L. Marshall[45], F. Menanteau[28,29], R. Miquel[30,46], E. Neilsen[4], A. A. Plazas[34], E. Sanchez[47], V. Scarpine[4], M. Schubnell[36], I. Sevilla-Noarbe[47], M. Smith[48], R. C. Smith[21], F. Sobreira[26,49], E. Suchyta[50], M. E. C. Swanson[29], G. Tarle[36], R. C. Thomas[20], D. L. Tucker[4], and A. R. Walker[21]
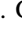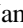
(DES Collaboration)

[1] Kavli Institute for Cosmological Physics, University of Chicago, Chicago, IL 60637, USA
[2] Department of Physics and Astronomy, University of Pennsylvania, Philadelphia, PA 19104, USA
[3] Harvard-Smithsonian Center for Astrophysics, 60 Garden Street, Cambridge, MA 02138, USA
[4] Fermi National Accelerator Laboratory, P.O. Box 500, Batavia, IL 60510, USA
[5] Department of Physics, Brandeis University, Waltham, MA 02453, USA
[6] Department of Astronomy, Indiana University, 727 E. Third Street, Bloomington, IN 47405, USA
[7] Department of Physics & Astronomy, University College London, Gower Street, London WC1E 6BT, UK
[8] Department of Physics, University of Chicago, Chicago, IL 60637, USA
[9] Enrico Fermi Institute, University of Chicago, Chicago, IL 60637, USA
[10] Astrophysical Institute, Department of Physics and Astronomy, 251B Clippinger Lab, Ohio University, Athens, OH 45701, USA
[11] The eScience Institute and the Department of Astronomy, University of Washington, Seattle, WA 98195, USA
[12] Oskar Klein Centre, Department of Physics, Stockholm University, SE-106 91 Stockholm, Sweden
[13] Department of Astronomy and Astrophysics, University of California Santa Cruz, 1156 High Street, Santa Cruz, CA 95064, USA
[14] Department of Astronomy, University of Illinois Urbana Champaign, 1002 W Green Street, Urbana, IL, 61801, USA
[15] Space Telescope Science Institute, 3700 San Martin Drive, Baltimore, MD 21218, USA
[16] Department of Physics and Astronomy, The Johns Hopkins University, 3400N. Charles Street, Baltimore, MD 21218, USA
[17] Instituto de Fisica Teorica UAM/CSIC, Universidad Autonoma de Madrid, E-28049 Madrid, Spain
[18] ARC Centre of Excellence for All-sky Astrophysics (CAASTRO), Mount Stromlo Observatory, Weston Creek, ACT 2611, Australia
[19] The Research School of Astronomy and Astrophysics, Australian National University, Canberra, ACT 2601, Australia
[20] Lawrence Berkeley National Laboratory, 1 Cyclotron Road, Berkeley, CA 94720, USA
[21] Cerro Tololo Inter-American Observatory, National Optical Astronomy Observatory, Casilla 603, La Serena, Chile
[22] Department of Physics and Electronics, Rhodes University, PO Box 94, Grahamstown, 6140, South Africa
[23] LSST, 933 North Cherry Avenue, Tucson, AZ 85721, USA
[24] CNRS, UMR 7095, Institut d'Astrophysique de Paris, F-75014 Paris, France
[25] Sorbonne Universités, UPMC Univ Paris 06, UMR 7095, Institut d'Astrophysique de Paris, F-75014, Paris, France
[26] Laboratório Interinstitucional de e-Astronomia—LIneA, Rua Gal. José Cristino 77, Rio de Janeiro, RJ—20921-400, Brazil
[27] Observatório Nacional, Rua Gal. José Cristino 77, Rio de Janeiro, RJ—20921-400, Brazil
[28] Department of Astronomy, University of Illinois, 1002 W. Green Street, Urbana, IL 61801, USA
[29] National Center for Supercomputing Applications, 1205 West Clark Street, Urbana, IL 61801, USA
[30] Institut de Física d'Altes Energies (IFAE), The Barcelona Institute of Science and Technology, Campus UAB, E-08193 Bellaterra (Barcelona), Spain
[31] Institute of Space Sciences, IEEC-CSIC, Campus UAB, Carrer de Can Magrans, s/n, E-08193 Barcelona, Spain
[32] Kavli Institute for Particle Astrophysics & Cosmology, P.O. Box 2450, Stanford University, Stanford, CA 94305, USA
[33] Department of Physics, California Institute of Technology, Pasadena, CA 91125, USA
[34] Jet Propulsion Laboratory, California Institute of Technology, 4800 Oak Grove Drive, Pasadena, CA 91109, USA
[35] Department of Astronomy, University of Michigan, Ann Arbor, MI 48109, USA
[36] Department of Physics, University of Michigan, Ann Arbor, MI 48109, USA
[37] SLAC National Accelerator Laboratory, Menlo Park, CA 94025, USA
[38] Department of Physics, ETH Zurich, Wolfgang-Pauli-Strasse 16, CH-8093 Zurich, Switzerland
[39] Center for Cosmology and Astro-Particle Physics, The Ohio State University, Columbus, OH 43210, USA
[40] Department of Physics, The Ohio State University, Columbus, OH 43210, USA
[41] Astronomy Department, University of Washington, Box 351580, Seattle, WA 98195, USA
[42] Australian Astronomical Observatory, North Ryde, NSW 2113, Australia
[43] Argonne National Laboratory, 9700 South Cass Avenue, Lemont, IL 60439, USA
[44] Departamento de Física Matemática, Instituto de Física, Universidade de São Paulo, CP 66318, São Paulo, SP—05314-970, Brazil
[45] George P. and Cynthia Woods Mitchell Institute for Fundamental Physics and Astronomy, and Department of Physics and Astronomy, Texas A&M University, College Station, TX 77843, USA
[46] Institució Catalana de Recerca i Estudis Avançats, E-08010 Barcelona, Spain
[47] Centro de Investigaciones Energéticas, Medioambientales y Tecnológicas (CIEMAT), Madrid, Spain
[48] School of Physics and Astronomy, University of Southampton, Southampton SO17 1BJ, UK
[49] Instituto de Física Gleb Wataghin, Universidade Estadual de Campinas, Campinas, SP—13083-859, Brazil
[50] Computer Science and Mathematics Division, Oak Ridge National Laboratory, Oak Ridge, TN 37831, USA

Abstract

The discovery of a kilonova (KN) associated with the Advanced LIGO (aLIGO)/Virgo event GW170817 opens up new avenues of multi-messenger astrophysics. Here, using realistic simulations, we provide estimates of the number of KNe that could be found in data from past, present, and future surveys without a gravitational-wave trigger. For the simulation, we construct a spectral time-series model based on the DES-GW multi-band light curve from the single known KN event, and we use an average of BNS rates from past studies of $10^3 \, \mathrm{Gpc^{-3} \, yr^{-1}}$, consistent with the one event found so far. Examining past and current data sets from transient surveys, the number of KNe we expect to find for ASAS-SN, SDSS, PS1, SNLS, DES, and SMT is between 0 and 0.3. We predict the number of detections per future survey to be 8.3 from ATLAS, 10.6 from ZTF, 5.5/69 from LSST (the Deep Drilling/Wide Fast Deep), and 16.0 from *WFIRST*. The maximum redshift of KNe discovered for each survey is $z = 0.8$ for *WFIRST*, $z = 0.25$ for LSST, and $z = 0.04$ for ZTF and ATLAS. This maximum redshift for *WFIRST* is well beyond the sensitivity of aLIGO and some future GW missions. For the LSST survey, we also provide contamination estimates from Type Ia and core-collapse supernovae: after light curve and template-matching requirements, we estimate a background of just two events. More broadly, we stress that future transient surveys should consider how to optimize their search strategies to improve their detection efficiency and to consider similar analyses for GW follow-up programs.

Key words: stars: neutron

1. Introduction

The first detection by aLIGO/Virgo of a gravitational-wave (GW) signal from a binary neutron star coalescence (Abbott et al. 2017a, 2017b) and the identification of the optical counterpart (Coulter et al. 2017; Soares-Santos et al. 2017; Valenti et al. 2017) marks the beginning of an exciting era of joint electromagnetic (EM) and GW studies. Optical counterparts from the mergers of a binary containing a neutron star are called "kilonova" (KN; see Metzger 2017 for a review and references therein). Theoretical studies predict that outflows of neutron-rich material during the merger enable *r*-process nucleosynthesis and that the decay of these *r*-process elements results in isotropic thermal emission. As KN events result in visible transients in the optical and infrared, with timescales of hours to days, Metzger & Berger (2012) have predicted that nearby KNe may be bright enough to find with modern optical telescopes. These predictions have been confirmed.

Optical observations of KNe can constrain theories about neutron star mergers, in particular identifying them as the progenitors of short gamma-ray bursts (GRBs). These events can also be used to measure the current expansion rate of the universe if there is a GW signal and the associated host galaxy redshift can be measured (e.g., Schutz 1986; Dalal et al. 2006). Additionally, untriggered KN discoveries in the optical would help LIGO re-evaluate past marginal signals and improve their detection algorithms.

To date, there have been a small number of inconclusive KN detections (e.g., Berger et al. 2013; Tanvir et al. 2013; Jin et al. 2016), none of which were triggered by a transient survey. With an optical counterpart of a GW event having been discovered, this event can be used to estimate the volumetric rate of KN events. Making the simplistic assumptions that all KN events are the same and that the volumetric rate is constant with redshift, we can predict how many of these events can be found in past, present, and future surveys. This is a follow-up of the work by Doctor et al. (2017), who considered a wide range of KN models and examined two seasons of data from the Dark Energy Survey Supernova Program (DES-SN). Here, we examine a single model, but a wide range of surveys. Other studies (e.g., Rosswog et al. 2017) have considered the detectability of KNe with future surveys based on estimated search depths, but here we consider depth, cadence, and area of the surveys using realistic observation libraries.

In this Letter, we use simulations to assess the capabilities of photometric surveys to discover KNe without a GW trigger. This is different from the follow-up mode for GW170817 and for past EM searches (Abbott et al. 2016b; Annis et al. 2016; Cowperthwaite et al. 2016; Soares-Santos et al. 2016) that followed a GW trigger from LIGO (Abbott et al. 2016b, 2016c, 2017a). Over the last decade there has been a large effort in predicting biases for SN Ia distance measurements that are used as cosmological probes (e.g., Scolnic et al. 2017), and this effort has resulted in increasingly realistic simulations. The SNANA (Kessler et al. 2009) software used for these studies has been applied to many cases beyond Type Ia supernovae, including core-collapse SNe, superluminous SNe and kilonovae (Doctor et al. 2017). All simulation and analysis tools used here are publicly available.[51]

In Section 2, we briefly review the KN discovery and use companion works to model the light curve and KN rate. In Section 3, we describe 11 optical surveys and our simulation methods. Results are presented in Section 4, along with estimates of the background contamination from SNe. Finally, in Section 5, we discuss future analyses to optimize these surveys and present conclusions in Section 6.

2. The Optical Counterpart to LV G298048

2.1. Discovery of Counterpart

Just over 11 hr after the aLIGO trigger (Abbott et al. 2017a, 2017b), the optical counterpart was found (Coulter et al. 2017; Soares-Santos et al. 2017; Valenti et al. 2017). The counterpart was identified as a point source located near NGC 4993. This galaxy is 40 Mpc away, with redshift $z = 0.0098$ (Kourkchi & Tully 2017). In a companion paper by Soares-Santos et al. 2017, we use our DECam (Flaugher et al. 2015) search data to show the likelihood that the transient is in fact directly connected to the GW event is >99%. We therefore rely on this event for our analysis.

---

[51] http://snana.uchicago.edu
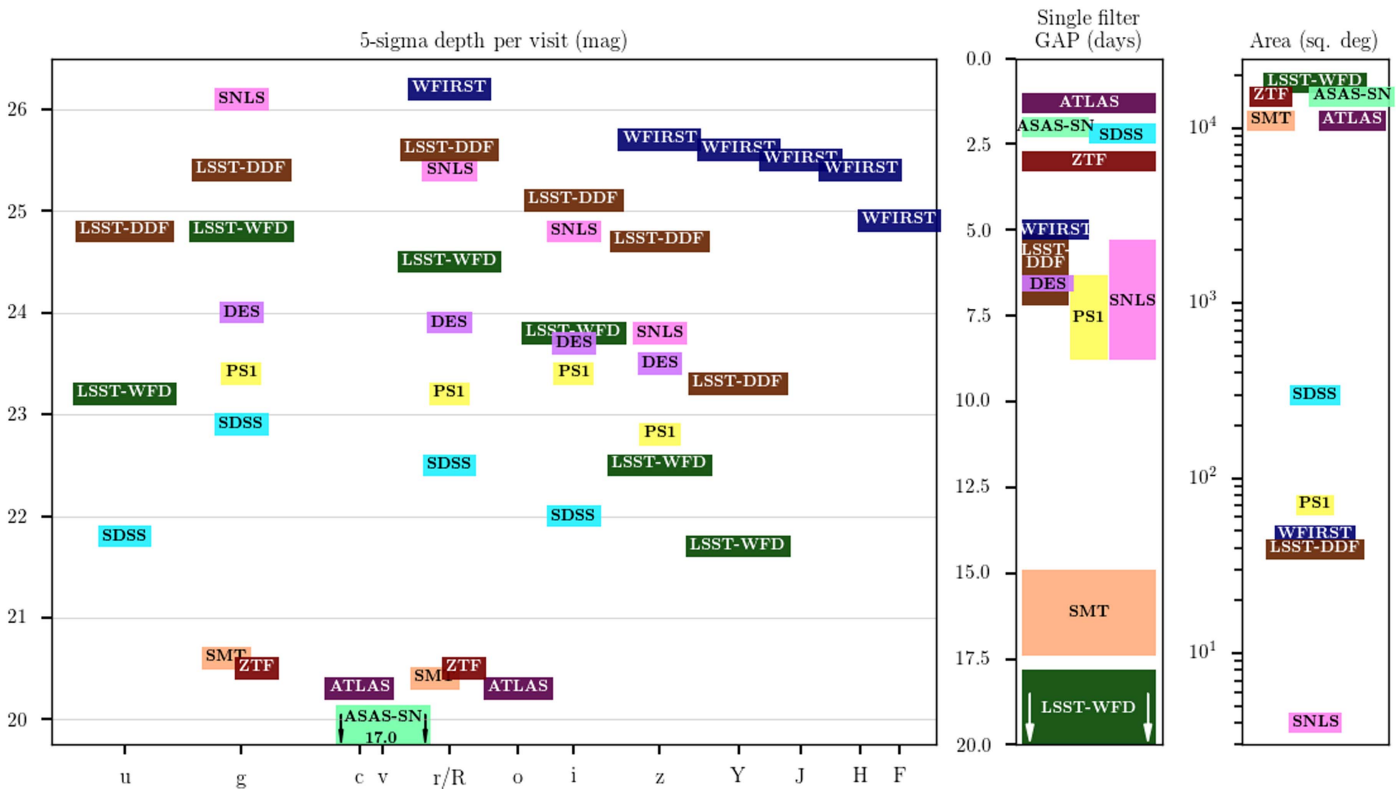
Figure 1. Display of key characteristics for *transient surveys* used in our analysis. Left panel: the depth per night per filter. Middle panel: the mean gap between repeat observations in a single filter. Right panel: the survey area covered each observing year. Numbers for each panel are given explicitly in Table 1.

Table 1
Summary Information for Each Survey

| Survey	Filters	Depths (5σ mag)	Cadences[a] (Days)	Area[b] (Deg²)	Duration[c] (Years)	Citation[d]
SDSS	*ugriz*	21.8, 22.9, 22.5, 22.	2.2, 2.2, 2.2, 2.2	300	2	Frieman et al. (2008)
SNLS	*griz*	26.1, 25.4, 24.8, 23.8	8.8, 6.3, 5.3, 8.5	4	5	Astier et al. (2006)
PS1	*griz*	23.4, 23.2, 23.4, 22.8	8.8, 8.7, 8.2, 6.3	70	4	Scolnic et al. (2014)
DES	*griz*	24.0, 23.9, 23.7, 23.5	6.8, 6.4, 6.3, 6.5	27	5	Kessler et al. (2015)
ASAS-SN	*V*	17.5	2	15000	5	Shappee et al. (2014)
SMT	*gr*	20.6, 20.4	17.4, 14.9	11000	5	Scalzo et al. (2017)
ATLAS	*co*	20.3, 20.3	1.3, 1.3	11000	5	Tonry (2011)
ZTF	*gr*	20.5, 20.5	3.0, 3.0	15000	5	Bellm (2014)
LSST DDF	*ugrizy*	24.8, 25.4, 25.6, 25.1, 24.7, 23.3	5, 6, 7, 7, 7, 7	40	10	LSST Science Collaboration et al. (2009)
LSST WFD	*ugrizy*	23.2, 24.8, 24.5, 23.8, 22.5, 21.7	30, 35, 18, 19, 21, 18	18000	10	LSST Science Collaboration et al. (2009)
WFIRST	*RZYJHF*	26.2, 25.7, 25.6, 25.5, 25.4, 24.9	5, 5, 5, 5, 5	45	2	Hounsell et al. (2017)

Notes.
[a] Mean duration between return visits in each filter.
[b] Total amount of sky area covered per year.
[c] Total number of years per survey.
[d] Describes observation history or characteristics.

2.2. KN Light Curve and Modeling

We model UV to NIR to allow for a broad range of analysis. While Doctor et al. (2017) showed that an NIR model is sufficient (e.g., *i* and *z* bands) for estimating KN detections, the bluer bands can be used to reject backgrounds from supernovae. Our KN model is determined using *ugrizY HK* photometry from the DES-GW papers (Cowperthwaite et al. 2017; Soares-Santos et al. 2017). To build a spectral model for simulations, we take the smoothed light curves from

Cowperthwaite et al. (2017) in *ugrizY HK* and "mangle" (Hsiao et al. 2007) a spectral time series to match the observed photometry. The mangling uses wavelength-dependent splines with knots at the effective wavelengths of the eight photometric filters. Our model has peak $i - z \sim 0.0$ and fades roughly 5 magnitudes over 7 days, in agreement with the data.

Cowperthwaite et al. (2017) show that this KN includes both a blue and red component, resulting in early time colors that are bluer than most models that predict $i - z \sim 1$ mag (e.g., Barnes et al. 2016). While our observed KN may not reflect the
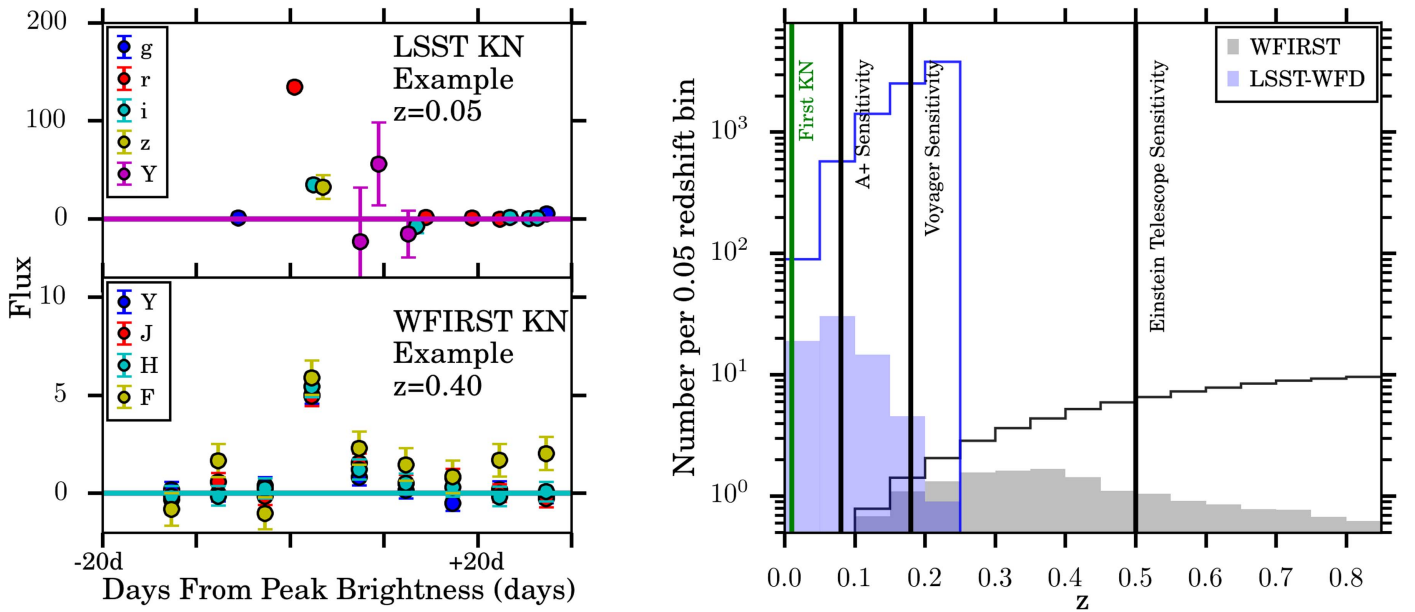
Figure 2. (Left) Example simulated KN light curves from LSST and *WFIRST* that pass our selection requirements. The vertical axis flux unit is defined such that $mag = 27.5 - 2.5 \log(Flux)$. (Right) KN redshift distributions for all events in the survey footprint (solid histogram) and for events passing selection requirements (shaded histogram). Green vertical line shows the KN redshift ($z = 0.0098$), and black vertical lines show the sensitivity of future GW experiments.

general population, we do not attempt to speculate about the population properties.

2.3. Estimate of Volumetric Rate

We use a constant volumetric KN rate of $10^3 \, \text{Gpc}^{-3} \, \text{yr}^{-1}$ as a conservative estimate based on a compilation of rates by Abbott et al. (2016a). This estimate is consistent with the fact that the LIGO O1 upper limit is $1.2 \times 10^4 \, \text{Gpc}^{-3} \, \text{yr}^{-1}$ (Abbott et al. 2016a), and O2 surveyed ~10 times more volume than O1, suggesting a rate of ~$10^3 \, \text{Gpc}^{-3} \, \text{yr}^{-1}$. Furthermore, this rate is broadly consistent with the aLIGO search time (<2 years) and search volume ~$(100 \, \text{Mpc})^3$.

3. Simulation of Transient Surveys

For this analysis, we have selected large surveys with the following criteria: they operate as rolling searches and have (or expect to have) discovered at least 100 SNe, an arbitrary limit. The compilation of surveys is listed in Table 1 and includes that from The Sloan Digital Sky Survey-II (SDSS; Frieman et al. 2008), Panoramic Survey Telescope and Rapid Response System (PS1; Kaiser et al. 2010,) Supernova Legacy Survey (SNLS; Astier et al. 2006), Dark Energy Survey (DES; Dark Energy Survey Collaboration et al. 2016), Skymapper Telescope (SMT; Scalzo et al. 2017), *Wide-Field Infrared Survey Telescope* (*WFIRST*; Spergel et al. 2015; Hounsell et al. 2017), The Large Synoptic Survey Telescope (LSST; LSST Science Collaboration et al. 2009), The Asteroid Terrestrial-impact Last Alert System (ATLAS; Tonry 2011), Zwicky Transient Facility (ZTF[52]; Bellm 2014),[53] and All-Sky Automated Survey for Supernovae (ASAS-SN; Shappee et al. 2014).

We use the SNANA simulation and analysis package (Kessler et al. 2009) to simulate each survey using filter

---

Table 2
Expected Number of KNe Found in Each Sample

| Survey	# KNe[a]	Survey Years	KN Redshift Range
SDSS	0.13	2	0.02–0.05
SNLS	0.11	4	0.05–0.20
PS1	0.22	4	0.03–0.11
DES	0.26	5	0.05–0.20
ASAS-SN	<0.001	3	...
SMT	0.001	5	0.01–0.01
ATLAS	8.3	5	0.01–0.03
ZTF	10.6	5	0.01–0.04
LSST WFD	69	10	0.02–0.25
LSST DDF	5.5	10	0.05–0.25
WFIRST	16.0	2	0.1–0.8

Note.
[a] Total for the entire duration of the survey.

transmission functions and a cadence library with a list of observation dates, where each date includes the observed zero point, sky noise, and point-spread function (PSF) measured from images. For SDSS, PS1, SNLS, and DES,[54] each cadence library has been created from the actual survey observations, and therefore includes genuine fluctuations from weather and operational issues. For LSST, the cadence library is computed[55] from the baseline cadence published by LSST using the Operations Simulator (Delgado et al. 2014), which uses historical weather data near Cerro Pachon to make realistic estimates of observational conditions and cadence. For *WFIRST* and SMT, we use the observation libraries based on Hounsell et al. (2017) and Scalzo et al. (2017), respectively.

---

[52] https://www.ptf.caltech.edu/page/ztf
[53] PTF does not have set cadence/depth so is not included here.

[54] Includes Deep and Shallow Fields, numbers listed here are average over all fields.
[55] Observations coadded nightly in Biswas et al. (2017) from "MINION_1016."
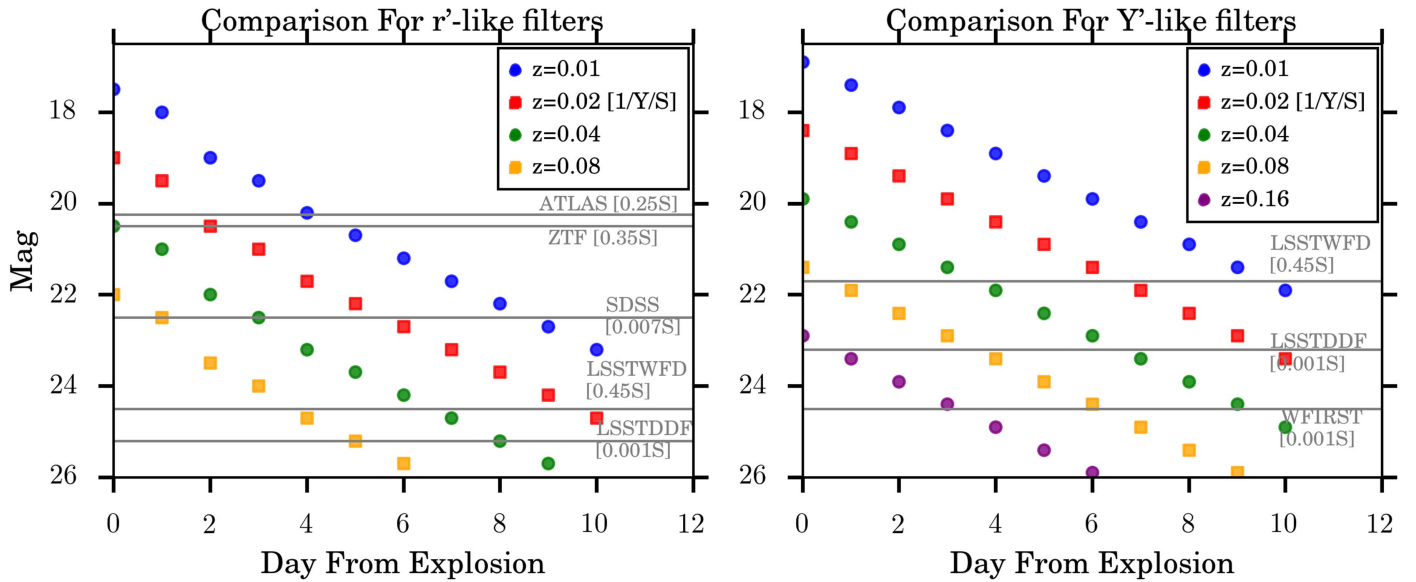
Figure 3. Synthetic KN light curves at different redshifts (see the legend) for LSST *r* band (left) and *Y* band (right). Horizontal lines indicate search depth for the labeled survey.

For ZTF,[56] ATLAS,[57] and ASAS-SN,[58] we use average quantities for the cadence, zero point, sky noise, and PSF. The resulting average-cadence libraries do not account for fluctuations from weather, but they are still useful for making forecasts. Global survey characteristics (depth, cadence, area, duration) are shown in Table 2 and illustrated in Figure 1. There is a dynamic range of 9 magnitudes between the shallowest (ASAS-SN) and deepest (SNLS, *WFIRST*) surveys, and the survey wavelengths extend from the ultraviolet (*u* band) to the infrared (*F* band—central wavelength of 1.8 μm). Figure 1 expresses the cadence as the average gap in time between observations with the same filter. We also show the amount of sky area covered, ranging from 4 deg^2 (SNLS) to 18,000 deg^2 (LSST).

We simulate KN detections in two steps. The first step is the trigger simulation, requiring two detections that are separated by at least 30 minutes to reject asteroids. A detection is characterized by the efficiency versus signal-to-noise ratio (S/N), and the efficiency is typically 50% at S/N = 5. The second step is the analysis, which uses the following selection requirements designed to reject supernova backgrounds.

1. At least two filter bands have at least one observation with S/N > 5. This requirement is largely redundant with the trigger.
2. The time period when transient measured with S/N > 5 is less than 25 days (30 days for *WFIRST*).
3. There is at least one observation within 20 days prior to the first S/N > 5 observation.
4. There is at least one observation within 20 days after the last S/N > 5 observation.

The second requirement explicitly rejects long-lived light curves. The last two requirements reject events that peak before or after the survey time window.

---

[56] The ZTF simulation done here is for the public survey (P. Nugent, private communication).
[57] J. Tonry, private communication.
[58] www.asas-sn.osu.edu

4. Results

The predicted number of KN detections for each survey is given in Table 2. In all of the existing data samples (SDSS, SNLS, PS1, DES, SMT), the expected number of events is well below unity, although the expected number is ∼0.7 if the KN totals from these four surveys are combined. Despite the wide variety of area, cadence, and depth, the predicted number of detections in SDSS, SNLS, PS1, and DES are all within a factor of ∼2.

For future surveys, the estimated rate is larger. As shown in Table 2, the number of KN discoveries from ATLAS and ZTF is ∼1–2 per year, due to their depth and rapid cadence. The number of discoveries from LSST WFD is ∼7 per year and from LSST DDF is ∼0.5 per year. Figure 2 (left) shows a discovered KN light curve for LSST WFD. Figure 2 (right) shows that LSST WFD can discover ∼0.8% of the KNe events in their footprint out to *z* = 0.25.

WFIRST has a shorter transient survey duration (2 years), but still finds as many KNe per season as LSST. This KN discovery potential is from a combination of depth, medium-sized area, and high red sensitivity. We find that the *WFIRST* efficiency is as high as ∼30% in its survey volume. Most interestingly, as shown in Figure 2, we see that *WFIRST* will discover KNe out to *z* = 0.8. Since *WFIRST* includes observations in the *H* and *F* bands, a KN with peak luminosity in the rest-frame *z* band can still be discovered at *z* ∼ 0.5 in these red filters.

To illustrate the interplay between depth, rate, and sky coverage, we show in Figure 3 the *r* and *Y* detection limits of multiple surveys overlaid on our KN light curve as it would appear at discrete redshifts.

4.1. Background Contamination from Supernovae

With 69 KN events expected for the LSST WFD survey, we now switch to simulating the background from supernova (SNe). We include Type Ia SNe (SN Ia) based on the SALT2-II spectral model (Betoule et al. 2014), and core-collapse (CC) SNe based on a library of 43 templates (Kessler et al. 2010).

In addition to the trigger and analysis requirements in Section 3, we use the PSNID fitting program (Sako et al. 2008) to select KN-like objects via light curve template matching. The templates include SN Ia, Type II SNe, Type Ib/c SNe, and our KN event. For a given simulated CC template, the corresponding template is removed from the PSNID fit so that we don't match a simulated CC template to itself. This PSNID analysis uses bands at all wavelengths, and thus even a KN flux limit in the bluer bands add useful information.

For the full 10 year survey, we generated nearly 200 million SNe (16% Ia, 84% CC), and find that 9 events are identified as a KN by PSNID. However, only 2 of these events have a reasonable fit-probability, $P_{fit} > 0.001$, where P_{fit} is computed from the χ^2 and number of degrees of freedom. This background is 2.9% of the number of KNe detected. We also calculate the frequency that KNe in our simulations are misclassified as SNe and find this happens only 0.05% of the time, though this number is likely optimistic because we use the same KN in our simulation and classification.

5. Discussion

None of the surveys discussed here have been optimized to find KNe, so the KN yields are expected to be low. SDSS, PS1, SNLS, LSST DDF, and *WFIRST* are all partially optimized for measurement of SN Ia light curves, which have typical durations of 60 days. While we expect ~1 KNe in past data sets, we note that it is unlikely to find such an event in light curve catalogs. Instead, a search for KNe in old data requires a re-analysis of all single-epoch detections to make less strict trigger cuts than those applied during past surveys. As improved volumetric KN rate estimates become available, all of our KN predictions can be re-scaled.

We have performed a preliminary study of SN background, and while this small (3%) background is encouraging, we note a few caveats that require further study. First, our simulations do not include potential contaminants from rare SN types, moving objects (asteroids), and non-SN transients such as orphan afterglows of GRBs (e.g., Singer et al. 2013) and M-dwarf flares (e.g., Hawley et al. 2014).

The second caveat is that we have implicitly assumed that all KN are the same, which is very unlikely to be correct. Ideally, our single KN template should be expanded to accept a wide range of KNe, perhaps with the aid of theoretical models such as Barnes et al. (2016). However, the challenge is to keep the SN backgrounds low while accepting a broader class of KN events.

Another caveat is that we have used the full end-of-survey light curves, but to get crucial follow-up observations with other instruments, KN events need to be efficiently identified within a few days of the merger event. Partial light curve studies will be needed to optimize KN target selection.

The final caveat is related to the KN host galaxies. In a recent search of DES-SN data (without a GW trigger), Doctor et al. (2017) found that image-subtraction artifacts increase the flux scatter well beyond what is expected from Poisson noise, and thus reduce the search sensitivity by a factor of 3 if all KNe occur inside their host galaxy. For KN events like this one, the event is well away from the galaxy center, as is expected for the majority of short GRBs (Fong et al. 2013). Therefore, image-subtraction artifacts are likely to be a subdominant issue, though the impact on expected KN should still be quantified.

One of the most interesting findings of this analysis is the ability for *WFIRST* to discover high-redshift KNe. This is particularly exciting because it would probe the cosmic history of NS mergers. Furthermore, it could provide an absolute distance scale to $z \sim 0.5$, which could be the first absolute distance measurement in between the local and cosmic microwave background (CMB) Hubble constant measurements. What is also illuminating is that *WFIRST* may detect KNe at higher redshift than the sensitivity of future GW missions. H.-W. Chen et al. (in preparation), based on methodology from Chen et al. (2017), estimate the sensitivity of next-generation gravitational-wave detectors, and we mark these sensitivities on Figure 2. We find that the LIGO upgrade A+ design, the future detector LIGO Voyager, and the planned Einstein Telescope all have sensitivity to GW triggers below the depth of *WFIRST* to KN events. Furthermore, theoretical models consistent with Cowperthwaite et al. (2017) suggest that the blue component depends on viewing angle, while the red component is isotropic. The IR capability of *WFIRST* may therefore have the additional advantage of better sensitivity to all viewing angles. There is an ongoing effort to design a joint GW and *WFIRST* program, called *GWFIRST*, optimized for NIR follow-up of GW detections.

Finally, this analysis only looks at survey detections without a GW trigger, whereas the most likely mode for most telescopes will be follow-up of announced GW events. With estimates of area, cadence, and observing conditions, all of the simulation tools used here can be used to optimize follow-up strategies.

6. Conclusion

We have used simulations to predict the number of KNe that can be found in past, present, and future data sets. The simulation uses a KN model that matches our DECam light curve data, and for each survey it uses realistic observation histories. We find that the expected number of events for every past survey is ~0–0.3 due to the small area, shallow depth, or sparse cadence, though combined can be up to ~1 event. For future surveys like LSST and *WFIRST*, we expect tens of KN discoveries. In particular, we find that *WFIRST* can find KNe at redshifts past planned GW sensitivities of future projects, opening up new possibilities of cosmological KN and NS science.

ORCID iDs

P. S. Cowperthwaite https://orcid.org/0000-0002-2478-6939
M. Soares-Santos https://orcid.org/0000-0001-6082-8529
J. Annis https://orcid.org/0000-0002-0609-3987
D. E. Holz https://orcid.org/0000-0002-0175-5064
E. Berger https://orcid.org/0000-0002-9392-9681
V. A. Villar https://orcid.org/0000-0002-5814-4061
P. Nugent https://orcid.org/0000-0002-3389-0586
F. J. Castander https://orcid.org/0000-0001-7316-4573
A. Drlica-Wagner https://orcid.org/0000-0001-8251-933X
D. Gruen https://orcid.org/0000-0003-3270-7644
R. A. Gruendl https://orcid.org/0000-0002-4588-6517
J. L. Marshall https://orcid.org/0000-0003-0710-9474
R. Miquel https://orcid.org/0000-0002-6610-4836
E. Sanchez https://orcid.org/0000-0002-9646-8198
G. Tarle https://orcid.org/0000-0003-1704-0781
A. R. Walker https://orcid.org/0000-0002-7123-8943

References

Abbott, B. P., Abbott, R., Abbott, T. D., et al. 2016a, ApJL, 832, L21
Abbott, B. P., Abbott, R., Abbott, T. D., et al. 2016b, PhRvL, 116, 241103
Abbott, B. P., Abbott, R., Abbott, T. D., et al. 2016c, PhRvL, 116, 061102
Abbott, B. P., Abbott, R., Abbott, T. D., et al. 2017a, PhRvL, 118, 221101
Abbott, B. P., Abbott, R., Abbott, T. D., et al. 2017b, PhRvL, 119, 161101
Annis, J., Soares-Santos, M., Berger, E., et al. 2016, ApJL, 823, L34
Astier, P., Guy, J., Regnault, N., et al. 2006, A&A, 447, 31
Barnes, J., Kasen, D., Wu, M.-R., & Mart'inez-Pinedo, G. 2016, ApJ, 829, 110
Bellm, E. 2014, The Third Hot-wiring the Transient Universe Workshop ed. P. R. Wozniak et al., 27
Berger, E., Fong, W., & Chornock, R. 2013, ApJL, 774, L23
Betoule, M., Kessler, R., Guy, J., et al. 2014, A&A, 568, A22
Biswas, R., Cinabro, D., & Kessler, R. 2017, SNANA simlib from MINION_1016 OpSim Outpu, Zenodo, doi:10.5281/zenodo.1006719
Chen, H.-Y., Holz, D. E., Miller, J., et al. 2017, arXiv:1709.08079
Coulter, D. A., Foley, R. J., Kilpatrick, C. D., et al. 2017, Sci, https://doi.org/10.1126/science.aap9811
Cowperthwaite, P. S., Berger, E., Soares-Santos, M., et al. 2016, ApJL, 826, L29
Cowperthwaite, P. S., Berger, E., Villar, V. A., et al. 2017, ApJL, 848, L17
Dalal, N., Holz, D. E., Hughes, S. A., & Jain, B. 2006, PhRvD, 74, 063006
Dark Energy Survey Collaboration, Abbott, T., Abdalla, F. B., et al. 2016, MNRAS, 460, 1270
Delgado, F., Saha, A., Chandrasekharan, S., et al. 2014, Proc. SPIE, 9150, 915015
Doctor, Z., Kessler, R., Chen, H. Y., et al. 2017, ApJ, 837, 57
Flaugher, B., Diehl, H. T., Honscheid, K., et al. 2015, AJ, 150, 150
Fong, W., Berger, E., Chornock, R., et al. 2013, ApJ, 769, 56
Frieman, J. A., Bassett, B., Becker, A., et al. 2008, AJ, 135, 338
Hawley, S. L., Davenport, J. R. A., Kowalski, A. F., et al. 2014, ApJ, 797, 121
Hounsell, R., Scolnic, D., Foley, R. J., et al. 2017, arXiv:1702.01747
Hsiao, E. Y., Conley, A., Howell, D. A., et al. 2007, ApJ, 663, 1187
Jin, Z.-P., Hotokezaka, K., Li, X., et al. 2016, NatCo, 7, 12898
Kaiser, N., Burgett, W., Chambers, K., et al. 2010, Proc. SPIE, 7733, 77330E
Kessler, R., Bassett, B., Belov, P., et al. 2010, PASP, 122, 1415
Kessler, R., Bernstein, J. P., Cinabro, D., et al. 2009, PASP, 121, 1028
Kessler, R., Marriner, J., Childress, M., et al. 2015, AJ, 150, 172
Kourkchi, E., & Tully, R. B. 2017, ApJ, 843, 16
LSST Science Collaboration, Abell, P. A., Allison, J., et al. 2009, arXiv:0912.0201
Metzger, B. D. 2017, LRR, 20, 3
Metzger, B. D., & Berger, E. 2012, ApJ, 746, 48
Rosswog, S., Feindt, U., Korobkin, O., et al. 2017, CQGra, 34, 104001
Sako, M., Bassett, B., Becker, A., et al. 2008, AJ, 135, 348
Scalzo, R. A., Yuan, F., Childress, M. J., et al. 2017, PASA, 34, e030
Schutz, B. 1986, Natur, 323, 310
Scolnic, D., Jones, D. O., Rest, A., et al. 2017, ApJ, submitted (arXiv:1710.00845)
Scolnic, D., Rest, A., Riess, A., et al. 2014, ApJ, 795, 45
Shappee, B. J., Prieto, J. L., Grupe, D., et al. 2014, ApJ, 788, 48
Singer, L. P., Cenko, S. B., Kasliwal, M. M., et al. 2013, ApJL, 776, L34
Soares-Santos, M., Holz, D. E., Annis, J., et al. 2017, ApJL, 848, L16
Soares-Santos, M., Kessler, R., Berger, E., et al. 2016, ApJL, 823, L33
Spergel, D., Gehrels, N., Baltay, C., et al. 2015, arXiv:1503.03757
Tanvir, N. R., Levan, A. J., Fruchter, A. S., et al. 2013, Natur, 500, 547
Tonry, J. L. 2011, PASP, 123, 58
Valenti, S., David, Sand, J., et al. 2017, ApJL, 848, L24